OPTIMAL PERFORMANCE OF MULTIPLE ENERGY SOURCES UNDER VARYING DISPATCH STRATEGIES ON A 4G BASE TRANSCEIVER STATION

*OLABODE, O.E., **AKINYELE, D.O., ***ARIYO, F.K., ****RAJI, A.A., *****OMONIYI, E.B., ******AKINDE, O.K
Department of Electrical and Information Engineering, Achievers University, Owo, Nigeria.
Department of Electrical and Electronics Engineering, Olusegun Agagu University of Science and Technology, Okitipupa, Nigeria.
Department of Electrical and Electronic Engineering, Obafemi Awolowo University, Ife, Nigeria.
Department of Electrical and Electronic Engineering, Federal University of Agriculture, Abeokuta, Nigeria.
Department of Mechanical Engineering, Bells University of Technology, Ota, Nigeria.
Department of Electrical and Biomedical Engineering, Abiola Ajimobi Technical University, Ibadan, Oyo State.
akinyelescholar@gmail.com

Abstract- The instability of grid supply and the high cost of diesel are the key drivers for alternative use of renewable energy resources for powering base transceiver stations (BTS). This paper, therefore, focused on the design and performance estimation of different energy systems for powering a BTS using a site in Oyo State, Nigeria as a case study. The study first considers the possibility of supplying the BTS through the photovoltaic (PV) array, before exploring the integration of a micro-gas (mGGen) generating system under different dispatch strategies such as load following (LFDS), cycle charging (CCDS) and combined dispatch (CDDS) approaches. The location's solar irradiance and ambient temperature alongside the BTS load profile served as input into the hybrid optimization of multiple energy resources simulation tool employed for estimating the capacities of PV, battery, and inverter cum the system performance. The PV array's yearly energy generation, the load served, and the unmet electric load were used to determine whether or not the mGGen should be integrated with the PV system for the load demand considered. For different daily demands of 546.44 and 162.44 kWh/d, results presented 200 and 60 kW PV arrays, 14,350 and 4,266 Ah battery banks, and 30 and 10 kW inverters, and 30 kW mGGen components. The contributions of the PV and the mGGen under the LFDS, CCDS, and CDDS are 3.19 - 33.7 % and 64.4 - 100 %, respectively, with no unmet load. The hybrid PV/mGGen under the LFDS and CCDS strategy gives a better performance in terms of realizing a high RE contribution and the highest fuel and emissions saved to the tune of 16,555 m^3/yr and 31,963 kg/yr, respectively, compared to 70,981 m^3/yr of gas and 137,042 kg/yr being consumed and emitted by running the BTS entirely on the mGGen system. The initial cost, cost of energy, and the net present cost of the hybrid systems range from $ 12,197 to $ 175, 339, $0.149 to $ 0.423, and $ 301,353 to $966,429, respectively.

Keywords- Dispatch Strategy, Base Transceiver Station, Micro-gas Resource, Photovoltaic Array, Emission

1. INTRODUCTION

The place of accessibility to a steady, stable, and reliable power supply in fostering sustainable socio-economic growth of any nation in the area of agriculture, transportation, communication, e-health, education, manufacturing, mining, and aviation among others cannot be undervalued [1-3]. It is also interesting to know that these core sectors of the economy cannot do without an effective communication system either for initiating new contracts, engaging in a cross-border dialogue with partners or prospective customers, communicating employment opportunities to the general public, or for day-to-day order of activities within the organization [4-7]. To buttress this assertion, Nigeria like many other countries around the world has witnessed an exponential rise in the deployment of internet-enabled smart devices alongside a surge in the number of mobile phone users [6]. Data gathered from the mobile telecommunication operators based on the subscribers' subscriptions showed that there are one hundred and seventy million mobile phone users in Nigeria, and out of this figure between 10 to 20% use smartphones which is approximately 25 to 40 million people while the rest of this figure uses traditional phones [8]. Also, from the global perspective, more than half of the world's population which is approximately four billion live with internet access powered by the BTS of the network operators or mobile service provider. These statistics revealed an appreciable improvement compared with what it used to be in the last six years where just a third portion of the world population is known to have internet access [9].

Furthermore, the improvement recorded in the area of access and use of mobile telephones in Nigeria, for instance, can be traced to a rise in the number of mobile network service providers as compared to what it used to be at the inception of the global system for mobile communication (GSM) in 2001. As of today, the prominent mobile network service providers in Nigeria include Airtel, Multilink, Globacom, MTN, Etisalat, and 9mobile among others [10]. Each of these operators has its separate BTS sites to meet the demand of providing wider network coverage. On the global view, there are over four million macro BTS sites with average energy consumption per site at 25 MWh yearly [11], and while in Nigeria alone, the number of BTS sites installed nationwide has increased from 30,000 to 53,460 in the last five years [12]. As a point of emphasis, the pieces of equipment at the BTS are energy sensitive devices, as it contains not only telecommunication-enabled devices but also an air interface device for the wireless network [10]. Hence, for effective and uninterrupted operation expected of equipment at this site, sustainable energy management cannot be compromised. Unfortunately, the energy supply from many of the national grids in sub-Saharan African countries is highly epileptic and in a worst-case scenario is grossly unavailable most especially in many remote locations across the country [13,14]. Consequently, advocating for alternative sources to complement the supply from the grid for powering BTS equipment becomes a promising option.

The Diesel or petrol-generating sets are widely deployed as a viable alternative to provide an uninterruptible power supply since its energy output is scalable, predictable, and independent of weather variability [4]. Diesel generators unlike petrol-fired generators are widely preferred for heavy-duty operation because of the cost savings in the long term, expanded life cycle, and better loading capacity [4]. This accounts for its wide deployment to energize the BTS sites both in cities and in many isolated rural communities. However, factors such as the high cost of operation and maintenance, rising cost of procurement of diesel, frequent theft of diesel by the site operators in addition to massive release of greenhouse gases and other contaminants into the atmosphere pose a threat to its continuous usage [15-17]. Also, the continued reliance on this energy option presents an environmental concern in terms of air and noise pollution to their immediate community [18]. Despite these challenges, it is increasingly difficult to phase out diesel-generating sets for powering BTS sites looking at the stochastic nature of many RES and the ease with which it can be hybridized with RES [4,19]. The environmental friendliness of RES makes them a desired energy option in realizing SDG-7(affordable clean energy for all) and this indeed has opened up diverse research directions in the field of micro and mini-grid development and adoption. However, utilization of single RES many a time leads to low energy delivery or non-availability at all due to RES' stochastic nature. This presents a reliability issue and explains why multiple-generating sources should be adopted to perform complementary roles to guarantee a steady and reliable energy supply [18-21].

However, if multiple energy sources are to be used, then the need for efficient energy management among these participating sources becomes a thing of concern if all the energy sources will be effectively utilized to guarantee a constant energy supply from the hybrid system. To this effect, dispatch strategies can be employed to ensure better utilization of RES in the hybrid system relative to other sources with high emission generation. Therefore, dispatch strategies are perceived as a set of well-defined rules to control the participation of generators and storage bank operations for the period when there is insufficient renewable energy to supply the associated loads [22, 23]. It can further be described as the energy exchange coordination between the generating sources, that is, photovoltaic and micro-gas generators, batteries, and the load [24]. In view of this, a detailed review of works is presented in Table 1. The sole aim is to reveal the extent of work that has been done, figure out the available dispatch strategies, identify possible areas of application of these dispatch strategies, and also perform comparative analysis using metrics such as system stability, reliability, and techno-economic-environmental analysis. It is also aimed to open up possible research gap in the area of energy management of BTS in Nigeria.

Table 1. Overview of areas of application of different dispatch strategies in hybrid energy management systems

Authors	Types of control/ dispatch strategies employed	Applied areas/Country	Optimal configuration	The outcome of the analysis
Uwineza *et al.*, (2022)[25]	-Cycle charging -Load-following -Proposed dispatch	Student service centre building at the University of California, USA	PV/FCs/BATT	The developed control strategy (PD) achieved zero unmet loads and presents the lowest NPC and COEL
Shezan *et al.*, (2022)[26]	-Load following, -Generator order, -Combined dispatch, -Cycle charging	Off-grid rural electrification Australia	DieselGen/PV/BATT/WT	-Load following strategy achieved the lowest NPC and LCOE. -It equally offered the best system stability & reliability compared with other strategies examined.
Emad, Hameed, and El-Fergany, (2021)[27]	-Load following, -Cycle charging,	Rural Electrification in Egypt	PV/WT/BATT/	- Using LPSP and COE; AI techniques outsmart LF and CC

	-AI algorithms (GWO, PSO & GA)			- Using the convergence curve, GWO outsmarts performs better PSO and GA
Ishraque, *et al.,* (2021)[28]	-Generator order, -Cycle charging, -Load following, - HOMER predictive dispatch -Combined dispatch	Offgrid application Bangladesh	DieselGen/PV/BATT/WT	Load following strategy offers a stable system response with the least NPC, LCOE, operation, and CO_2 emission.
Jufri *et al.,* 2021)[29]	- Load following, -cycle charging -Combined dispatch - Optimal BES discharge	Off-grid application in Indonesia	DieselGen/PV/BES	OBD offered the least LCOE compared with other dispatch strategies investigated.
(Rezk *et al.,* 2021)[30]	-Load following -Cycle charging -Combined dispat., -Predictive strategy	Off-grid application in Saudi Arabia	PV/DieselGen/BATT	A predictive dispatch strategy was adjured as the best energy management system for the proposed off-grid electrification.
(Ishraque *et al.,* 2021)[31]	-HOMER predictive dispatch, -Load following, -Generator order, -Cycle charging, -Combined dispatch	Off-grid application in Kushighat, Bangladesh	WT/PV/BAT/DieselGen	Load following showed superior performance in terms of reduced LCOE, NPC, and CO_2 discharged
Arévalo *et al.,* (2020)[32]	-Load following, -Cycle Charging, -Custom Dispatch	Rural Electrification in Ecuador	PV/BATT/Hydrokinetic	Custom dispatch achieved the lowest NPC and LCOE when compared with other dispatch strategies.
Murugaperumal *et al.,* (2020)[33]	-Load following, -Cycle charging -Combined strategy	Offgrid application in Korkadu, India	Biomass/WT/PV/BATT	A combined dispatch strategy was adjured to give the best fit for the energy mix for the hybrid energy systems proposed.
Ramesh *et al.,* (2020)[34]	-Load following, -Cycle charging -Combined dispatch	Village Electrification in India	PV/WT/Hydro/DieselGen/BATT	The most optimal cost of operation was achieved using a combined dispatch strategy.
Micangeli *et al.,* (2020)[35].	-Load-following -Cycle charging - Predictive strategy (Mixed-integer linear programming)	Off-grid rural electrical in Kenya	PV/DieselGen/BATT	Both the load following and cycle charging approaches offered the least computational time making them suitable for sub-optimal design while the proposed predictive strategy is suitable for optimal performance though it exhibited a higher computational time.
Aziz, et al., (2019)[36]	-Combined dispatch -Load following -Cycle charging	Off-grid rural electrification in Iraq	PV/DieselGen/BATT	The least value of NPC and COE was obtained with a combined dispatch strategy relative to others.
Shezan, *et al.,* (2019)[37]	-Load following, -Cycle charging, -Generator order -Combined dispatch	Off-grid rural electrification in South Australia	PV/WT/DieselGen/BATT	Load following achieved the lowest value for NPC, COE, and CO2 discharged and by inference, it has optimum performance relative to other dispatch strategies.

A critical examination of the review presented in Table 1 showed that a good number of these dispatch strategies have been tailored towards achieving good energy management in hybrid energy systems designed for off-grid rural electrification. However, areas such as the health care sector, the agricultural sector, and base transceiver stations among others where efficient energy management is highly required have received less attention. To this effect, this current work employed the prominent dispatch strategies: load following strategy (LFDS), cycle charging strategy (CCDS), and combined dispatch strategy (CDDS) to achieve optimized energy from a hybrid of PV/mGGen designed for the BTS. The LFDS is a dispatch mechanism whose set of rules ensures that charging the storage bank or serving the deferrable load is left to the renewable power sources in the hybrid system while the generator (diesel or gas) is operated to generate enough energy to meet the primary load only. In CCDS, the generator operates on full power output purposefully to serve the primary loads while the excess after supplying the associated loads is used for charging the storage bank and also to power deferrable loads on the hybrid system. The CDDS on the other hand is a unique combination of both the LFDS and CCDS. It is simply the integration of both the load-following strategy and cycle charging strategy to meet the load requirement on the hybrid system. The major contributions of this current study to the canon of knowledge are;

i) a detailed review of existing works on the adoption of different dispatch strategies for energy management in hybrid energy systems for different areas of applications.
ii). proposed, designed, and simulated the performance of a hybrid of PV/mGGen under LFDS, CCDS, and CDDS for effective energy management on a 4G base transceiver station
iii). A detailed sensitivity analysis was carried out to evaluate the fuel saving and emission cut-down with different sizes of solar photovoltaic systems.

The rest of this paper is as sectioned thus, section 2 presents the methods and materials, section 3 majors on the results and discussion section, and section 4 presents the conclusion and recommendation based on the study.

2. METHODS

2.1. Description of BTS use as a case study

The coordinate of the base transceiver station used as the case study on the global positioning system is Lat. 7.8430° N, Long. 3.9368° E. It is a 4G enabled AIRTEL base transceiver situated within the palace of Alaafin of Oyo, Nigeria. The front view elevation of this BTS is shown in Fig.1

Fig. 1. 4G AIRTEL base transceiver station at Alaafin Palace, Oyo, Nigeria

2.2. Site load estimation and load profile

To be able to develop good hybrid energy systems for this BTS, there is a need for adequate estimation of the BTS loads and the development of an appropriate BTS load profile that will sufficiently capture the hourly operating characteristics of the telecommunication sites over the 24-hour time scale. The energy consumption by each appliance is a function of the product of appliance-rated capacity in watts and time of operation in hours usually throughout 24-hour time scale. This energy consumption per appliance is mathematically represented by Eqn (1) and to obtain all hourly energy consumed by the appliance over the day, Eqn.(2) is employed.

$$E_c = Appliance\ rated\ capacity\ (W) \times Time\ of\ operation(h) \quad (1)$$

$$E_{THC} = \sum_{i=1}^{24} E_{c_i} \quad (2)$$

Where: E_c = Energy consumed (Wh), E_{THC} = Total hourly energy consumed over a 24-hour time scale, E_{c_i} = Hourly energy consumption.

The load consumption of this BTS is shown in Table 2, which has been obtained from the site visit and the nameplate attached to each equipment. Table 2 specifies the appliance-rated capacity (W), duration of operation (usually on a 24-hour time scale), the daily demand in (kWh/day), including the manufacturer of the appliances. It can be seen that a good number of outdoor telecommunication sites come with an internal cooling system that is aided by atmospheric natural cooling, hence, the need for the installation of air-conditioning systems is inconsequential and highly uneconomical. Table 2 also presents the duration of operation of the equipment at the BTS sites. It was observed that some of the equipment are engaged over the 24-hour time scale while the lighting fitting and the aviation light are operated only for 12 hours and by inference, the lighting fittings as well as aviation light are put into use during the night time alone usually from 6 pm to 6 am. The total daily load demand of the BTS including the rectifier is 546.44 kWh/d while the daily load demand without the rectifier system is 162.44 kWh/d.

Table 2. Load requirement of a typical 4G enabled BTS

S/N	BTS system component	Vendor model	Power rating (W)	No. of units	Total power rating (W)	Duration of operation/day (hr)	Daily demand (kWh/day)
1	Transmission Radio	Huawei	720	1	720	24	17.28
2	RF Antenna	Huawei	N/A	-	-	-	-
3	Sector	Huawei	N/A	-	-	-	-
4	1800 MHz RRU	Huawei	1000	3	3000	24	72
5	900 MHz RRU	Huawei	1000	3	3000	24	72
6	Rectifier	Huawei	16000	1	16000	24	384
7	Lighting fittings	Ericsson	36	2	72	12	0.864
8	Aviation fittings	Ericsson	25	1	25	12	0.3
Total					**22817**		**546.44**

2.3. Solar energy data for the case study

The PV array's performance depends to a large extent on the location's solar energy and the ambient temperature where the PV modules are to be implemented. The location's average solar irradiation [13] and the ambient temperature under consideration are shown in Figure 2 and 3, respectively, as obtained from HOMER environment based on the NASA surface meteorology and meteoblue database for the Oyo Alaafin location.

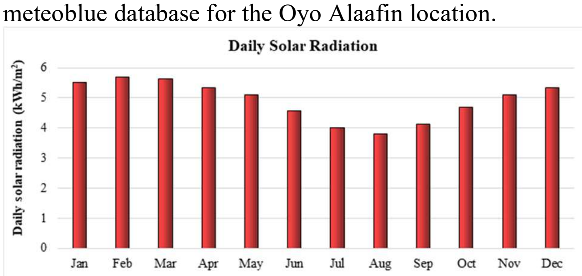

Fig 2. Study location daily solar irradiation

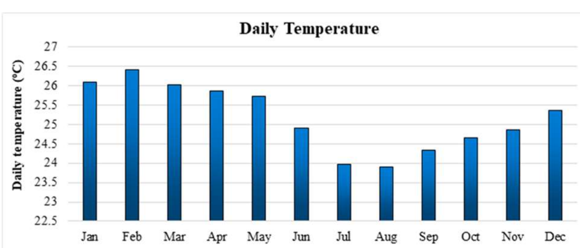

Fig 3. Study location daily temperature

2.4. Mathematical Modeling of Components of Hybrid Energy Systems

2.4.1. Solar photovoltaic array model

The power output of the solar photovoltaic array may be calculated by using Equations (3) and (4) [29, 39]:

$$P_S = n \cdot P_m \cdot d_r \cdot \frac{G_s}{G_{stc}} \cdot [1 + \gamma(\mathrm{T}_{\mathrm{cell}} - \mathrm{T}_{\mathrm{cell,stc}})] \qquad (3)$$

$$T_{cell} = AB_{temp} + \frac{(NOCT - 20℃)}{G_{ref}} \cdot G_s \qquad (4)$$

Where; $P_s, n, P_m, d_r, G_s, \gamma, T_{cell}, G_{stc}, NOCT, T_{cell,stc}, G_{ref}$ and AB_{temp} represents the PV array power output, power of a single PV panel, derate ratio, solar irradiance of the location, temperature coefficient of power, PV cell temperature, solar irradiance at STC of 1000 W/m^2, nominal operating cell temperature, cell temperature at STC, reference solar irradiance of 800 W/m^2, and the location's ambient temperature.

2.4.2. Modeling of battery bank capacity

The size of the battery may be calculated by employing Equation (5) [40]:

$$B_{Size} \frac{E_D \times D_A}{DOD \times V_{dc} \times \eta_b} \qquad (5)$$

Where; B_{Size}, E_D, D_A, V_{dc}, DOD, and η_b represents the size of the battery in ampere-hours, average daily maximum demand, the days of autonomy, nominal system voltage (DC), battery depth of discharge, and battery bank's efficiency, respectively.

2.4.3. Modeling of inverter size

Eqn (6) [23] is employed to calculate the inverter's capacity. In order to accommodate the inductive load's starting current, the inductive load capacity is multiplied by a factor of 3, while the addition of resistive load and the inductive load capacity is then multiplied by a factor of 1.25 [40]:

$$I_{VS} = 1.25 \times [P_{RE} + (3 \times (P_{IND}))] \qquad (6)$$

where; I_{VS}, P_{RE}, and P_{IND} represent the inverter size, total resistive load, and total inductive loads, respectively.

2.4.4. Modeling of micro-gas generator capacity

The capacity of the generator whether diesel or gas-fired is usually higher than the peak load and this is usually achieved by multiplying the peak load with a factor depending on the design. The total load requirements largely determine the size of the generator to be deployed and the amount of fuel consumed by the generator can be computed using Eqn (7)[40];

$$Gen_{FC} = \propto Y_{Gen} + \beta P_{Gen} \quad (7)$$

Where; Gen_{FC}, $\propto$, β, Y_{Gen}, and P_{Gen} are the generator fuel consumption, fuel curve coefficient of the generator, fuel curve slope of the generator, rated capacity of the generator, and the output power of the generator, respectively.

2.4.5. Cost analysis

The HOMER tool's economic evaluation is based on the net present cost (NPC). NPC of a system or system component describes the present value of the all costs associated with installation and operation of the said system component over the project lifespan, with the present value (PV_l) of all the revenues that it generates over the project lifespan being deducted. NPC then includes the capital, replacement, and operation and maintenance (O and M) costs, etc. NPC is therefore computed in HOMER simulation environment by adding the total discounted cash flows yearly over the project lifespan. The methodology for the cost analysis in this paper is obtained from the HOMER library. The total annualized cost, C_{tac} represents the annualized value of the total NPC, C_{tNPC}, which may be computed using Eqn. (8):

$$C_{tac} = \mathrm{CRF}\,(i, P_{lf}) \cdot C_{tNPC} \quad (8)$$

where: C_{tNPC}, i, P_{lf}, and CRF represents the total NPC ($), the annual real discount rate (%), the project lifespan, and a function that returns the capital recovery factor. C_{tac} is used to compute the cost of energy (COE) produced. CRF is essentially a ratio that defines the PV_l of a series of equal cash flows on a yearly basis (i.e., annuity) is defined by Eq. (9):

$$\mathrm{CRF}\,(i, N_Y) = \frac{i(1+i)^{N_Y}}{(1+i)^{N_Y}-1} \quad (9)$$

Where; N_Y is the number of years. PV_l may be described as the current equivalent worth of a set of future cash flows considering the the time value of money. Also, the real discount rate, i may be computed using Eq. (10):

$$i = \frac{i_n - f}{1+f} \quad (10)$$

Where; i_n and f represent the nominal discount rate, i.e., the rate at which money is being borrowed, and the rate of inflation that is being expected.

The cost of energy (COE) in its own case represents the cost per kWh, i.e., cost per unit of useful electricity being generated by the system. Eq. (11) may be used to compute COE:

$$\mathrm{COE} = \frac{C_{tac} - C_{bl}\mathrm{T_{LS}}}{\mathrm{E_{LS}}} \quad (11)$$

Where; C_{bl}, T_{LS}, and E_{LS} represents boiler's marginal cost ($/kWh), total thermal load being served (kWh/yr), and the total electric load being served (kWh/yr), respectively. In the case of this paper, the PV and the natural gas generator are assumed, and they do not serve a thermal load; therefore, T_{LS}= 0.

2.4.6. Performance evaluation metrics

The comparative performance of the three dispatch strategies deployed in this study was assessed using the amount of load served by the energy-generating sources in the single-source and the hybrid configurations, the volume of natural gas fuel consumed, and the quantity of gas emission metrics. The main idea driving such a comparative study is the need to ascertain the best energy option for the 4G-enabled BTS under investigation.

3. RESULTS AND DISCUSSION

This section discusses the simulation results obtained for the proposed energy system for the 4G-enabled BTS under different dispatch strategies - LFDS, CCDS, and CDDS. The simulation tools used in this study are Hybrid Optimization of Multiple Energy Resources (HOMER) and the Microsoft Excel software. The HOMER software was used for the simulation analysis while the Microsoft Excel software was used for the preparation of tables and results.

3.1. Load profile for 4G base transceiver site

The load requirement for the 4G-enabled BTS equipment presented in Table 2 was input into HOMER software to generate the daily load profile for the study under consideration, as shown in Figure 4. Two load profiles were presented: the load with a rectifier and the load without a rectifier. This idea is introduced in this work to have two different options as it may not sound practicable to run a 16-kW rectifier system on a PV-based single-source energy supply.

For the profile with a 16-kW rectifier, the baseline average daily load demand is 546.44 kWh/day, while the value of the average load, peak load, and load factor are 22.77 kW, 22.82 kW, and about 100 %, respectively. However, for the profile without the 16-kW profile, the baseline average daily load demand is 162.44 kWh/day, while the value of the average load, peak load, and load factor are 6.77 kW, 6.82 kW, and 99 %, respectively.

It is clear from Figure 4 that the difference between the day and night energy consumption is the 12-hour period in the day when the lighting fitting and the aviation light are not operated.

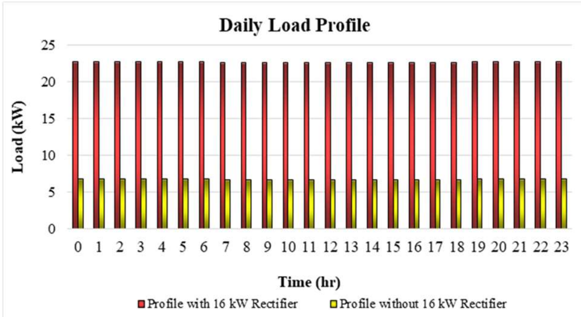

Fig. 4. Daily load profile for the 4G base transceiver sites

The total yearly demand of the BTS for the two cases - with and without the 16 kW rectifier is 199,450.6 and 59,290.6 kWh/yr, respectively, obtained by multiplying the daily demands by 365 days in the year. These values give an idea of the daily and annual load demand on the site that the proposed energy system will be required to support. For an in-depth comparative performance analysis of the energy systems under varying dispatch strategies, different scenarios were simulated such as follows - solar PV only under the LFDS, CCDS, and CDDS, and solar PV and micro-gas generator (mGGen) under the LFDS, CCDS, and CDDS.

3.2. Solar PV output performance under LFDS, CCDS, and CDS

The system topology used for the simulation the solar PV with battery bank and inverter supplying the 4G BTS loads (with and without the 16-kW rectifier) are shown in Figure 5(a) and 5(b),

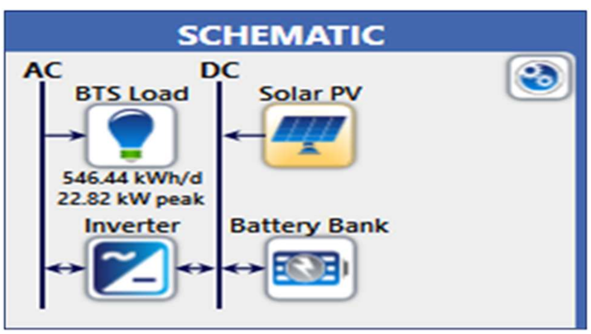

Fig. 5(a). System topology with PV-only configuration (BTS load with 16 kW rectifier)

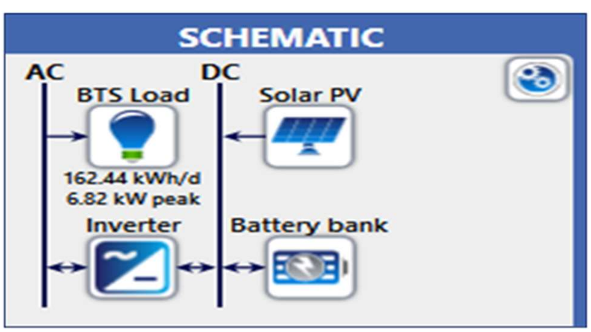

Fig. 5(b). System topology with PV only configuration (BTS load without 16 kW rectifier)

while the average monthly energy output from the solar PV array is shown in Figure 6(a) and 6(b). The simulation analysis at this point centers on determining the required sizes of the PV array, battery, and inverter, as well as evaluating the output energy from the PV array. The whole essence is to be able to establish the amount of the 4G-enabled BTS loads that can be served under each of these dispatch strategies.

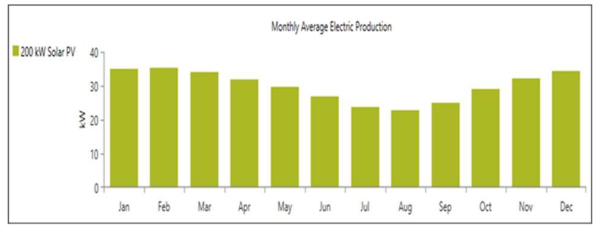

Fig. 6(a). Average monthly energy output from 200 kW PV for a profile with 16 kW rectifier

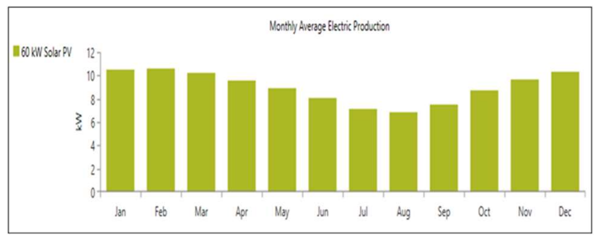

Fig. 6(b). Average monthly energy output from 60 kW PV for a profile without a rectifier

Result analysis of the two scenarios presented in Figure 6 showed that the corresponding inverter sizes for the profiles was found to be about 30 and 10 kW, in a situation where there are no inductive loads identified; the battery capacities are 14,350 Ah and 4,266 Ah. These are obtained at days of autonomy, battery efficiency, depth of discharge, and the nominal voltage of 1.5, 85 %, 70 %, and 96 V DC, respectively. It is clear from Figures 6 (a) and (b) that the months of February and August have the maximum and the minimum monthly generation.

This is because February and August are in dry and rainy seasons, respectively. The corresponding values of the monthly average generation for these two months - which are the maximum and the minimum production of the 200 kW-rated PV system are about 37 and 24 kW, while the values of about 11 and 6.7 kW are obtained for the 60 kW-rated PV system. The annual output energy obtained under different strategies was reported in Tables 4 and 5 for the two profiles and for the 200 kW PV system with the 16-kW rectifier under the LFDS and CCDS, the yearly energy production is 262,472 kWh/yr with an unmet load of 7.08 %. However, the unmet load obtained under the CDDS is 26.1 %. The unmet loads of 7.08 and 26.1 % imply that the BTS demand will not be met for about 620 and 2,286 hours in the year - i.e., about 26 and 95 days in the year. The obtained results demonstrate that either the LFDS or the CCDS is suitable for the 200 kW PV power system for the BTS compared to the CDDS option.

In the case of the 60 kW PV for the profile without a rectifier, the same energy generation and unmet load of

78,742 kWh/yr and 4.33 % are obtained for the three strategies. An unmet load of 4.33 % implies that the BTS will not be served for about 379 hours (i.e., around 16 days) in the year. This means that any of the strategies may be suitable for the case of a 60 kW PV system for the BTS system, as the output performance parameters - annual energy output, and inverter size (for the profile without rectifier) are the same. Therefore, the PV system operated either under the LFDS or the CCDS may be selected as a suitable option for effective energy management of any of the 4G-enabled BTS load profiles (with and without a rectifier).

Table 3. Result of simulation for the profile with 16 kW rectifier

Performance Parameters (Profile with 16kW Rectifier)	**LFDS**	**CCDS**	**CDDS**
PV capacity (kW)	200	200	200
Energy production (kWh/yr)	262, 472	262, 472	262,472
Unmet load (kWh/yr)	14,116 (i.e.,7.08 %)	14,116 (i.e.,7.08 %)	52, 046 (i.e., 26.1 %)

Table 4. Result of simulation for the profile without 16 kW rectifier

Performance Parameters (Profile with 16 kW Rectifier)	**LFDS**	**CCDS**	**CDDS**
PV capacity (kW)	60	60	60
Energy production (kWh/yr)	78, 742	78,742	78,742
Unmet load (kWh/yr)	2,569 (i.e.,4.33 %)	2,569 (i.e.,4.33 %)	2,569 (i.e.,4.33 %)

3.3. Hybrid PV/mGGen for 4G BTS Load

The performance of a single-source energy system presented above shows that none of the strategies was able to achieve zero unmet loads for the 200 and 60-kW PV systems. Also, achieving zero unmet loads will lead to an unnecessary increase in the size of the PV arrays. For this reason and the need to ensure that all the load requirements are satisfied, this study considers the option of integrating another source with the existing solar PV array.

The existing PV system is then hybridized with a micro-gas generator (mGGen) system. The hybrid system configuration is shown in Figure 7, which was used to analyze the impact of these three dispatch strategies (LFDS, CCDS, and CDDS). In the case of the hybrid configuration, this study considers all the loads - i.e., the profile with the 16-kW rectifier. Therefore, the PV and mGGen systems shown in Figure 7 have been simulated for the daily demand of 546.44 kWh/day.

The optimal size of mGGen obtained from the HOMER simulation is 30 kW, which can also satisfy the load without any contribution from the PV array.

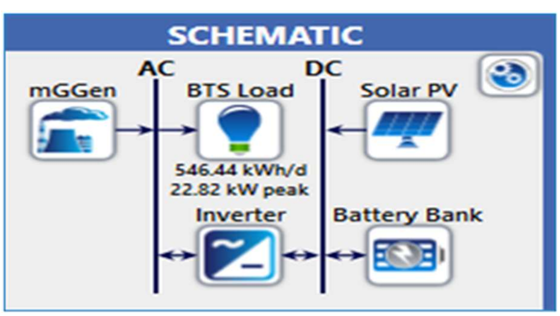

Fig.7. Hybrid PV/mGGen system for the 4G-enabled BTS load

3.4. Performance of the Hybrid PV/mGGen

The monthly average energy generation from this hybrid configuration under LFDS is shown in Figure 8, which reveals monthly energy generation by each energy source in the hybrid systems for different sizes of solar PV array and 30 kW mGGen. The size of the mGGen is such that can satisfy the load requirements of the BTS with or without the PV array - i.e., it can support a peak load of 22.82 kW. This is expected to offer a higher reliability during the rainy season when there is low contribution from the PV array.

Figures 8(a), (b), (c), (d), (e), (f), (g), and (h) represent 60 kW-PV and 30 mGGen; 50 kW-PV and 30 mGGen; 40 kW PV and 30 mGGen; 30 kW-PV and 30 mGGen, 20 kW-PV and 30 mGGen, 10 kW-PV and 30 mGGen, 5 kW-PV and 30 mGGen, and 0 kW-PV and 30 mGGen. The lower the contribution of the PV system, the higher the operation of and energy generation from the 30kW mGGen.

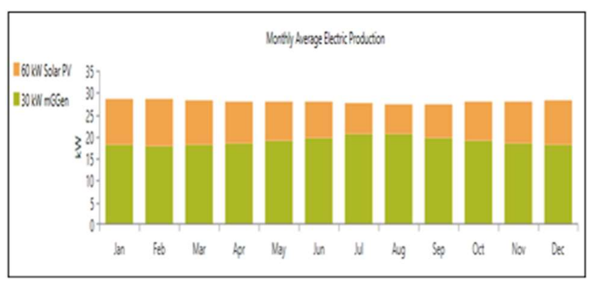

Fig 8(a). Monthly average energy generation by 60 kW-PV and 30 kW mGGen under LFDS

Fig 8(b). Monthly average energy generation by 50 kW-PV and 30 kW mGGen under LFDS

Fig.8(c). Monthly average energy generation by 40 kW-PV and 30 kWmGGen under LFDS

Fig.8 (d): Monthly average energy generation by 30 kW-PV and 30 kW mGGen under LFDS

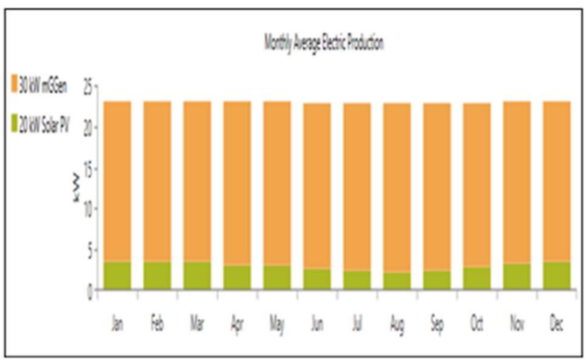

Fig 8(e): Monthly average energy generation by 20 kW-PV and 30 kW mGGen under LFDS

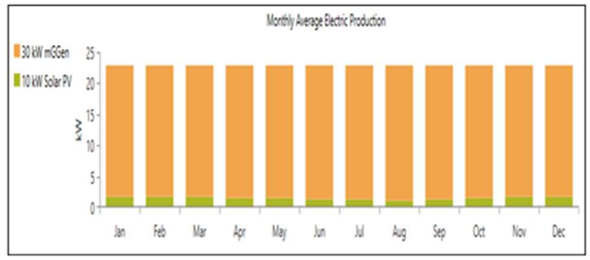

Fig 8(f). Monthly average energy generation by 10 kW-PV and 30 kW mGGen under LFDS

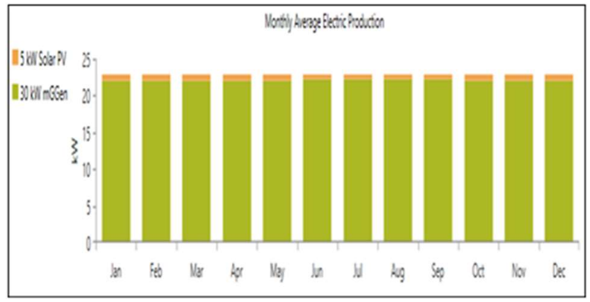

Fig 8(g). Monthly average energy generation by 5 kW-PV and 30 kW mGGen under LFDS

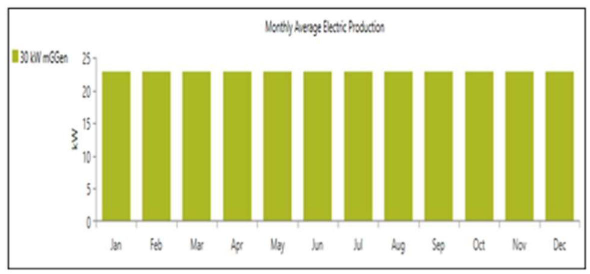

Fig.8(h). Monthly average energy generation by 0 kW-PV and 30 kW mGGen under LFDS

The percentage contributions of these hybrid systems are presented in detail in Table 5.

Table 5. Simulation results for PV and mGGen system under LFDS, CCDS and CDDS

PV size (kW)	mGGen size (kW)	Energy generated by PV (kWh/yr)	Energy generated by mGGen (kWh/yr)	% contribution by PV	% contribution by mGGen	Gas consumed (m^3/yr)	Strategy
60	30	78,742	142,365	35.6	64.4	54,426	LFDS
		78,742	142,365	35.6	64.4	54,426	CCDS
		78,742	154,557	33.8	66.2	54,998	CDDS
50	30	65,618	146,755	30.9	69.1	55,699	LFDS
		65,618	146,755	30.9	69.1	55,699	CCDS
		65,618	162,714	28.7	71.3	57,902	CDDS
40	30	52,494	152,861	25.6	74.4	57,470	LFDS
		52,494	152,861	25.6	74.4	57,470	CCDS
		52,494	173,279	23.3	76.7	61,663	CDDS
30	30	39,371	162,181	19.5	80.5	60,172	LFDS
		39,371	162,181	19.5	80.5	60,172	CCDS
		39,371	190,796	17.1	82.9	67,899	CDDS
		26,247	174, 517	13.1	86.9	63,750	LFDS
20	30	26,247	174,517	13.1	86.9	63,750	CCDS

		26,247	199, 452	11.6	88.4	70,981	CDDS
10	30	13, 124	186,985	6.56	93.4	67,366	LFDS
		13,124	186, 985	6.56	93.4	67,366	CCDS
		13,124	199, 452	6.17	93.8	70,981	CDDS
5	30	6,562	193,218	3.28	96.7	69,173	LFDS
		6,562	193,218	3.28	96.7	69,173	CCDS
		6,562	199,452	3.19	96.8	70,981	CDDS
-	30	-	199,452	-	100	70,981	LFDS
		-	199,452	-	100	70,981	CCDS
		-	199,452	-	100	70,981	CDDS

3.5. Fuel Consumption and Emission Analysis

Results presented in Table 5 also reveal the size of PV and mGGen hybrid systems, energy generated by each source, their percentage contributions, and the gas consumed under the three different dispatch strategies. The results show that the system operated under LFDS and CCDS has the same results with high PV contribution compared to the CDDS. Also, the fuel consumption of the system operated under the CDDS is high compared to those operated under the LFDS and CCDS.

This trend follows for all the hybrid systems; however, the same results were obtained when the 30 kW mGGen system is operated under the LFDS, CCDS, and CDDS. The maximum gas consumed by the 30 kW mGGen is 70,981 m^3/yr, which is the baseline for quantifying the amount of fuel saved by different hybrid systems. The estimated amount of gas saved by the 60-kW PV systems is 70,981 m^3/yr for the single-source systems options. This indicates that the 200 kW PV system will save more than the value of emissions saved by the 60 kW PV. The 60-kW PV a single source achieved 16,555 m^3/yr and 105,079 kg/yr as saved in fuel and amount of CO_2 respectively.

Table 6 provides the details of the fuel saved by different PV sizes (i.e., 5 to 60 kW PV system), while the amount of carbon dioxide gas saved by systems for different strategies are shown in Tables 7 and 8. The emissions saved are reported in terms of the following: carbon dioxide (CO_2), carbon monoxide (CO), unburned hydrocarbon (UH), particulate matter (PM), sulfur dioxide (SO_2) and nitrogen oxides (NO_X) as obtained from the HOMER simulation tool.

The minimum and maximum emissions are obtained for the 60 kW PV and 30 kW mGGen hybrid system and the 30 kW mGGen system. For the results presented in Table 8 for LFDS, the minimum values of CO_2, CO, UH, PM, SO_2, and NO_X were obtained for the 60 kW PV and 30 kW mGGen, which are 105,079, 349, 0, 9.95, 0, and 741 kg/yr, respectively, while the maximum values of 137,042, 456, 0, 12.8, 0, and 956 kg/yr were obtained for the 30 kW mGGen system.

Similarly, for the CDDS, the values of 106, 183, 353, 0, 9.95, 0, and 741 kg/yr, and 137,042, 456, 0, 12.8, 0, and 956 kg/yr were obtained for the 60 kW PV and 30 kW mGGen, and the 30 kW mGGen systems, respectively. It is observed that the hybrid system - 60 kW and 30 kW mGGen produced the lowest emissions when operated under the LFDS and CCDS compared to when operated under the CDDS. However, under the CDDS, the emissions for 20 kW PV and 30 kW mGGen, 10 kW PV and 30 kW mGGen, and the 5 kW PV and 30 kW mGGen systems are the same with the the values obtained when the BTS is being run with the 30 kW mGGen system. It is also evident that running the BTS entirely on a 30 kW mGGen produced the highest emissions. Therefore, using the results presented in Tables 7 and 8, the carbon dioxide emissions saved will be the difference between the highest value (137,042 kg/yr) and the lowest value (105,079 kg/yr), which is 31, 963 kg/yr. It is also obvious that the integration of the PV system with the 30 kW mGGen system provides an environmental benefit of avoiding or saving some amount of fuel and of course carbon emissions.

Table 6. Fuel consumed and fuel saved for PV and mGGen system under LFDS, CCDS, and CDDS

System size	% PV Contribution	% mGGen Contribution	Gas consumed (m^3/yr)	Gas saved (m^3/yr)	Strategy
60 kW PV and 30 kW mGGen	35.6	64.4	54,426	16,555	LFDS
	35.6	64.4	54,426	16,555	CCDS
	33.8	66.2	54,998	15,983	CDDS
50 kW PV and 30 kW mGGen	30.9	69.1	55,699	15,282	LFDS
	30.9	69.1	55,699	15,282	CCDS
	28.7	71.3	57,902	13,079	CDDS
40 kW PV and 30 kW mGGen	25.6	74.4	57,470	13,531	LFDS
	25.6	74.4	57,470	13,531	CCDS
	23.3	76.7	61,663	9,318	CDDS
30 kW PV and 30 kW mGGen	19.5	80.5	60,172	10,809	LFDS
	19.5	80.5	60,172	10,809	CCDS
	17.1	82.9	67,899	3,082	CDDS
	13.1	86.9	63,750	7,231	LFDS
	13.1	86.9	63,750	7,231	CCDS

20 kW PV and 30 kW mGGen	11.6	88.4	70,981	0	CDDS
10 kW PV and 30 kW mGGen	6.56	93.4	67,366	3,615	LFDS
	6.56	93.4	67,366	3,615	CCDS
	6.17	93.8	70,981	0	CDDS
5 kW PV and 30 kW mGGen	3.28	96.7	69,173	1,808	LFDS
	3.28	96.7	69,173	1,808	CCDS
	3.19	96.8	70,981	0	CDDS
30 kW mGGen	-	100	70,981	0	LFDS
	-	100	70,981	0	CCDS
	-	100	70,981	0	CDDS

Table 7. Emissions generated PV and mGGen system under LFDS and CCDS

Emission	**60 kW PV and 30 kW mGGen**	**50 kW PV and 30 kW mGGen**	**40 kW PV and 30 kW mGGen**	**30 kW PV and 30 kW mGGen**	**20 kW PV and 30 kW mGGen**	**10 kW and 30 kW mGGen**	**5 kW PV and 30 kW mGGen**	**30 kW mGGen**
CO_2	105,079	107,537	110,955	116,174	123,081	130,061	133,551	137,042
CO	349	358	369	386	409	432	444	456
UH	0	0	0	0	0	0	0	0
PM	10.5	10.1	10.4	10.9	11.5	12.2	12.5	12.8
SO_2	0	0	0	0	0	0	0	0
NO_X	733	750	774	811	859	907	932	956

Table 8. Emissions generated PV and mGGen system under CDDS

Emission	**60 kW PV and 30 kW mGGen**	**50 kW PV and 30 kW mGGen**	**40 kW PV and 30 kW mGGen**	**30 kW PV and 30 kW mGGen**	**20 kW PV and 30 kW mGGen**	**10 kW and 30 kW mGGen**	**5 kW PV and 30 kW mGGen**	**30 kW mGGen**
CO_2	106,183	111,789	119,051	131,092	137,042	137,042	137,042	137,042
CO	353	372	396	436	456	456	456	456
UH	0	0	0	0	0	0	0	0
PM	9.95	10.5	11.2	12.3	12.8	12.8	12.8	12.8
SO_2	0	0	0	0	0	0	0	0
NO_X	741	780	831	915	956	956	956	956

3.6. Cost Analysis

The cost analysis for the different system configurations is presented in Table 9 based on the HOMER simulation. The discount rate, inflation rate, annual capacity shortage, and the project lifetime of 8 %, 2 %, 10 %, and 25 years, respectively have been assumed for the economic analyses. The costs of solar panel per Watt, inverter per kW, a 12 V 200 Ah battery, and the natural gas-based generator per kW were obtained from [41-44]. The analysis also assumes the addition of 10 % of the cost of components in the HOMER model, which accounts for the system installation.

For the PV, the initial capital, replacement, and O and M input to the software are $ 1, 650/kW, $ 1,650/kW, and $ 10/yr; the corresponding values for the battery component are $ 178.2/ unit, $178.2/unit, and $ 10/yr; the values for the inverter are $108.9/kW, $108.9/kW and $ 1/yr; and the values used for the natural gas-operated gen are $405.56/kW, $ 405.56/kW and $0.6/hour, respectively.

It is clear from the results shown in Table 9 that the systems' costs obtained under the LFDS and the CCDS are the same, these are consistent with the results previously reported in Tables 6, 7 and 8. However, relatively higher costs are obtained when the systems are being run under the CDDS. The capital cost of PV systems decreases with the size of PV, with the minimum and maximum values of $ 8,250 and $ 330, 000 for the 5 kW PV and 30 kW mGGen and the 200 kW PV systems, respectively.

The initial cost decreases with the size of the PV also. This is due to huge capital associated with the implementation of the PV system. The lowest and the highest initial capital are $12,197 and $ 558,878, for the 30 kW mGGen and the 200 kW PV systems, respectively. The trend of results for the net present cost (NPC) for the systems is that it decreases with the size of the PV also. The minimum cost of $223, 486 was obtained for the 60 kW PV under the CDDS, while the same maximum NPC of $ 966,429 was obtained for the 200 kW PV system for all the strategies.

The NPC for the 60 kW PV system is also lower than the values obtained for the 30 kW mGGen system because of the O and M and the fuel cost that are included in the case of the 30 kW natural gas generator over the project life. The cost of energy (COE) per kWh for the 60 kW PV was $ 0.384 under CDDS, which was lower than the same value of $ 0.423 obtained for the system under the LFDS and CCDS. The same value of COE of $ 0.403 was obtained for the 200 kW PV system under all the strategies.

Generally, the COE tends to reduce with the size of PV modules but with the systems operated under the CDDS having relatively higher values compared to those operated under the LFDS and CCDS. The operating cost also has the same trend with the COE, while the operating and maintenance (O and M) cost values are similar.

The fuel consumption and the fuel cost increase as the PV sizes are decreased. These parameters are also consistent with the results presented in Tables 7 and 8, the emissions generated, for instance, are found to be proportional to the gas consumed. The minimum and the maximum fuel consumption are 54,426 m^3 and 70,981 m^3, respectively, for the 60 kW PV and 30 kW mGGen systems. The corresponding lowest and highest fuel costs are $ 16,328 and $ 21,294.

The cost evaluation does not consider the cost of the control strategy components; however, the reported results can provide an idea about the trend of the cost parameters for analysis purposes and the understanding of the economic performance of the PV system. Also, the results obtained, especially the technical aspects, provide insights into what may likely be the performance of the control strategies in real-life situation should the system be implemented. This aspect will form a basis for future research work that will not only process the cost of control mechanism but also ascertain and examine the appropriate mathematical models for the LFDS, CCDS and the CDDS in details.

Table 9. Results of the cost analysis for the systems under the LFDS, CCDS and CDDS

System	Initial Cost ($)	Operating Cost ($)	Capital Cost ($)	NPC ($)	COE ($)	O and M ($)	Fuel Consumed (m^3)	Fuel Cost ($)	Strategy
60 kW PV (Without Rectifier)	175,339	9,748	99,000	301,353	0.423	-	-	-	LFDS
	175,339	9,748	99,000	301,353	0.423	-	-	-	CCDS
	138,273	6,592	99,000	223,486	0.384	-	-	-	CDDS
200 kW PV (With Rectifier)	558,878	31,526	330,000	966,429	0.403	-	-	-	LFDS
	558,878	31,526	330,000	966,429	0.403	-	-	-	CCDS
	558,878	31,526	330,000	966,429	0.403	-	-	-	CDDS
60 kW PV and 30 kW mGGen	124,810	24,859	99,000	446,168	0.173	5,256	54,426	16,328	LFDS
	124,810	24,859	99,000	446,168	0.173	5,256	54,426	16,328	CCDS
	163,934	23,721	99,000	435,739	0.169	4,070	54,998	16,499	CDDS
50 kW PV and 30 kW mGGen	108,310	25,141	82,500	433,314	0.168	5,256	55,699	16,710	LFDS
	108,310	25,141	82,500	433,314	0.168	5,256	55,699	16,710	CCDS
	112,586	24,821	82,500	433,465	0.168	4,286	57,902	17,370	CDDS
40 kW PV and 30 kW mGGen	91,810	25,572	66,000	422,388	0.164	5,256	57,470	17,241	LFDS
	91,810	25,572	66,000	422,388	0.164	5,256	57,470	17,241	CCDS
	96,086	26,310	66,000	436,213	0.169	4,565	61,663	18,499	CDDS
30 kW PV and 30 kW mGGen	75,310	26,283	49,500	415,077	0.161	5,256	60,172	18,052	LFDS
	75,310	26,283	49,500	415,077	0.161	5,256	60,172	18,052	CCDS
	79,586	28,744	49,500	451,173	0.175	5,027	67,899	20,370	CDDS
20 kW PV and 30 kW mGGen	58,810	27,256	33,000	411,159	0.159	5,256	63,750	19,125	LFDS
	58,810	27,256	33,000	411,159	0.159	5,256	63,750	19,125	CCDS
	58,810	29,425	33,000	439,203	0.170	5,256	70,981	21,294	CDDS
10 kW PV and 30 kW mGGen	42,310	28,240	16,500	407,388	0.158	5,256	67,366	20,210	LFDS
	42,310	28,240	16,500	407,388	0.158	5,256	67,366	20,210	CCDS
	42,310	29,325	16,500	421,410	0.163	5,256	70,981	21,294	CDDS
5 kW PV and 30 kW mGGen	34,060	28,733	8,250	405,503	0.157	5,256	69,173	20,752	LFDS
	34,060	28,733	8,250	405,503	0.157	5,256	69,173	20,752	CCDS
	34,060	29,275	8,250	412,514	0.160	5,256	70,981	21,294	CDDS
30 kW mGGen	12,197	28,737	-	383,701	0.149	5,256	70,981	21,294	LFDS
	12,197	28,737	-	383,701	0.149	5,256	70,981	21,294	CCDS
	12,197	28,737	-	383,701	0.149	5,256	70,981	21,294	CDDS

3.7. Variability in solar energy resource

Seasonal variations of the solar energy resource are a part of the factors that affect the solar PV systems performance. This is because the dry season in Nigeria benefits from good sunshine compared to the rainy season when cloudy days are being experienced. It is also important to state that the ambient temperature also changes with seasons, which is why it is critical to examine variation in temperature. With the assumption that the BTS worst-case load demand still remains 546.44 kWh/d, it is possible to ascertain what impact will a change in the solar irradiation of the location have on the system's performance. This study examines the effect of increasing and decreasing the solar insolation and temperature values by 25 % on the 60 kW PV and 30 kW mGGen. Figures 10 (a) and 10 (b) shows the initial solar radiation level, the solar energy resource that is 25 % lower than the initial solar radiation (lower level) and the solar radiation that is 25 % higher than the initial solar radiation (upper level). New simulations are then run in HOMER environment to determine the impact of changes in the location's solar radiation.

The simulation results for changes in the solar radiation are shown in Table 10. The results reveal that the PV generation is proportional to the solar radiation values; i.e., the percentage PV contributions of the 60 kW PV system with the lower solar radiation values are lower than the values obtained for the initial solar radiation values (initial level).

This is consistent with the fact PV devices that the higher the solar radiation, the higher the short-circuit current and of course, the maximum power current of the PV module, leading to an increase in the module's maximum power output, and vice-versa [45]. The contributions of the 60 kW PV system are quite higher than those of the initial level when the upper solar radiation values were used. This trend reverses with the percentage contribution of the 30 kW natural-gas operated generator (mGGen), as its contributions increase when the solar radiation values were reduced, and vice-versa.

The highest cost of energy, COE of the system is obtained when the solar irradiation is lowered, the same trend goes for the NPC. The operating cost, fuel consumed, fuel cost and the CO_2 emitted follow the same trend as the system with the upper solar radiation level present the lowest fuel consumption, fuel cost and emissions. The NPC, COE, fuel consumed, fuel cost and CO_2 emissions values obtained for the upper solar radiation level under the CDDS are the lowest of all the results. This shows that examining the variation in solar energy resource can present results that can provide deeper insights into the PV performance for better decision-making.

The simulation results for variation in temperature of the location are shown in Table 11. The lowest PV and the highest mGGen contributions are obtained for upper temperature level under the CDDS. However, the highest PV and the lowest mGGen contributions are reported for lower temperature level under the LFDS and CCDS. This may be explained from the fundamental knowledge of PV devices that PV modules are characterized at a standard test condition (STC) of 25°C.

Therefore, increasing the ambient temperature beyond this value leads to a decrease in the PV module's open circuit voltage leading a reduction in the module's maximum power output, while reducing the temperature below this value increases the open-circuit voltage and hence, the module's maximum power output [46, 47]. The changes in the fuel consumption, fuel cost and other costs, and the emissions are detailed in Table 11, and it is clear that variation in temperature of the location can also affect the performance of the PV system.

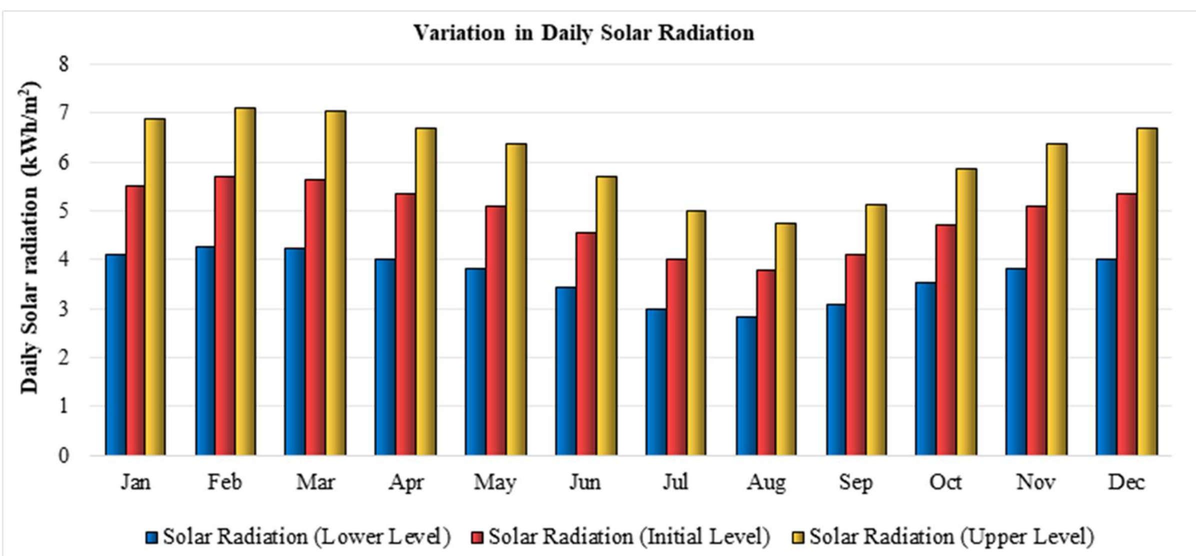

Fig. 10(a). The initial solar radiation and ambient temperature with lower and upper values

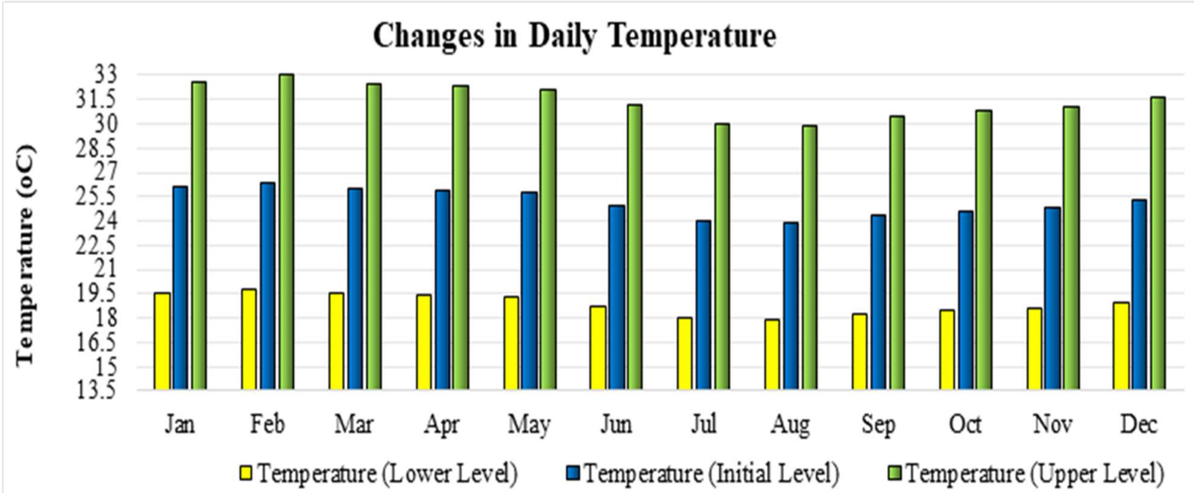

Fig.10(b). The initial ambient temperature and the lower and upper temperature values

Table 10. Results for changes in solar energy of the location under LFDS, CCDS and CDDS compared with the initial results (temperature unchanged)

System	% PV Contribution	% mGGen Contribution	Initial Cost ($)	NPC ($)	Operating Cost ($)	COE ($)	Fuel Consumed (m^3)	Fuel Cost ($)	CO_2 Emitted (kg/yr)	Strategy
60 kW PV and	28.1	71.9	124, 810	457,971	25,772	0.178	57,469	17, 241	110, 954	LFDS
30 kW mGGen	28.1	71.9	124,810	457,971	25,772	0.178	57,469	17, 241	110, 954	CCDS
(Lower Solar Radiation Level)	26	74	129,086	465,052	25, 998	0.180	60,490	18, 147	116, 787	CDDS
60 kW PV and	42.1	57.9	126, 235	450, 522	24,311	0.171	52, 055	15, 616	100, 501	LFDS
30 kW mGGen	42.1	57.9	126, 235	450, 522	24,311	0.171	52, 055	15, 616	100, 501	CCDS
(Upper Solar Radiation Level)	40.9	59.1	129, 086	410,005	21,370	0.159	50, 177	15, 053	96,875	CDDS
60 kW PV and	35.6	64.4	124, 810	446, 168	24,859	0.173	54, 426	16, 328	105, 079	LFDS
30 kW mGGen	35.6	64.4	124,810	446, 168	24,859	0.173	54, 426	16, 328	105, 079	CCDS
(Initial **Solar Radiation Level)**	33.8	66.2	163, 934	435, 739	23,721	0.169	54, 998	16, 499	106, 183	CDDS

Table 11. Results for changes in daily temperature of the location under LFDS, CCDS and CDDS compared with the initial results (solar radiation unchanged)

System	% PV Contribution	% mGGen Contribution	Initial Cost ($)	NPC ($)	Operating Cost ($)	COE ($)	Fuel Consumed (m^3)	Fuel Cost ($)	CO_2 Emitted (kg/yr)	Strategy
60 kW PV and	36.5	63.5	126, 235	448,901	24,960	0.174	54,215	16,265	104,672	LFDS
30 kW mGGen	36.5	63.5	126, 235	448,901	24,960	0.174	54,215	16,265	104,672	CCDS
(Lower Daily Temp. Level)	34.7	65.3	129, 086	433,011	23,510	0.168	54, 488	16, 346	105, 199	CDDS
60 kW PV and	34.7	65.3	126,235	450,575	25,089	0.175	54,647	16, 394	105, 506	LFDS
30 kW mGGen	34.7	65.3	126,235	450,575	25,089	0.175	54,647	16, 394	105, 506	CCDS
(Upper Daily Temp. Level)	32.7	67.3	129,086	438,856	23,962	0.170	55,580	16, 674	107,307	CDDS
60 kW PV and	35.6	64.4	124, 810	446, 168	24,859	0.173	54, 426	16, 328	105, 079	LFDS
30 kW mGGen	35.6	64.4	124,810	446, 168	24,859	0.173	54, 426	16, 328	105, 079	CCDS
(Initial Daily Temp. Level)	33.8	66.2	163, 934	435, 739	23,721	0.169	54, 998	16, 499	106, 183	CDDS

3.8. Future work

Future research study will consider the possibility of integrating additional renewable energy resources with the PV system both grid-connected and off-grid scenarios, including the evaluation of employing advanced battery technologies such as Lithium ion, ZEBRA, Vanadium Redox Battery (VRB), etc [48-52].

4. CONCLUSION

This paper has discussed the design and performance evaluation of different small-scale generating systems for supplying electricity to a 4G base transceiver station (BTS), given the need for a reliable electricity supply for telecommunications application. The impact of such energy solutions is to lower carbon emissions compared to when the load is being run entirely on a natural gas resource. The study first explored the possibility of supplying the BTS load from a solar photovoltaic (PV) array before considering the hybrid configuration of PV and a micro-gas (mGGen) power-generating system under different dispatch strategies such as the LFDS, CCDS, and CDDS approaches.

Two load profiles were also used as the basis of analysis for the single-source (PV only) option, while the profile with the rectifier device was used for analysis in the hybrid configuration. The solar PV array's yearly energy generation, the load served, and the unmet electric load were used to determine whether or not the mGGen should be integrated with the PV array system for the BTS load demand under consideration. The peak load and the daily demand of the BTS for the profile with and without the 16-kW rectifier are 22.82 kW and 546.44 kWh/day and 6.82 kW and 162.44 kWh/yr, respectively.

The simulation results show that the sizes of the PV array required are 200 and 60 kW for the two load profiles while the corresponding inverter sizes for these profiles are about 30 and 10 kW; the battery capacities are 14,350 Ah and 4,266 Ah, respectively. These were obtained at days of autonomy, battery efficiency, depth of discharge, and the nominal voltage of 1.5, 85 %, 70 %, and 96 V DC, respectively. Further analysis showed that the 200 kW PV system operated under the LFDS and CCDS produced the same energy of 262,472 kWh/yr with an unmet load of 7.08 %, while an unmet load obtained under the CDDS was 26.1%.

The obtained results demonstrate that either the LFDS or the CCDS is suitable for the 200 kW PV power system for the BTS compared to the CDDS option. In the case of the 60 kW PV system, the same energy generation and unmet load of 78,742 kWh/yr and 4.33 % were obtained for the three strategies. The result implies that any of the strategies may be suitable for the case of 60 kW PV system for the BTS system, as the output performance parameters - annual energy output, and inverter size (for the profile without rectifier) are the same. Therefore, the PV system operated either under the LFDS or the CCDS may be selected as a suitable option for the BTS.

The maximum gas consumed by the 30 kW mGGen is 70,981 m^3/yr, which was the baseline for quantifying the amount of fuel saved by different hybrid systems. Therefore, the amount of carbon dioxide emissions saved by 60 kW PV systems was 16,555 kg/yr. The minimum and the maximum emissions were obtained for the 60 kW PV and the 30 kW mGGen hybrid system and the 30 kW mGGen system, respectively. For LFDS, the minimum values of CO_2, CO, UH, PM, SO_2, and NO_X were obtained for the 60 kW PV and 30 kW mGGen, which are 105,079, 349, 0, 9.95, 0, and 741 kg/yr, respectively, while the maximum values of 137,042, 456, 0, 12.8, 0, and 956 kg/yr were obtained for the 30 kW mGGen system.

Similarly, for the CDDS, the values of 106, 183, 353, 0, 9.95, 0, and 741 kg/yr, and 137,042, 456, 0, 12.8, 0, and 956 kg/yr were obtained for the 60 kW PV and 30 kW mGGen, and the 30 kW mGGen systems, respectively. It was observed from the hybrid system - 60 kW and 30 kW mGGen produced lower emissions when operated under the LFDS and CDDS compared to when operated under the CDDS.However, under the CDDS, the emissions for 20 kW PV and 30 kW mGGen, 10 kW PV and 30 kW mGGen, and the 5 kW PV and 30 kW mGGen systems are the same with the the values obtained whhen the BTS is being run with the 30 kW mGGen system.

The results revealed that the carbon dioxide emissions saved will be the difference between the highest value (137,042 kg/yr) and the lowest value (105,079 kg/yr), which is 31, 963 kg/yr. The initial cost, cost of energy, and the net present cost of the hybrid systems range from \$ 12,197 to \$ 175, 339, \$0.149 to \$ 0.423, and \$ 301,353 to \$966,429, respectively. The impact of variation in solar energy of the location on the energy system is also reported. This study can be used for a better understanding of PV/micro-gas generating power systems for standalone applications such as the BTS system that does not depend on the grid.

Acknowledgement

The authors are grateful to Vritansh Technologies &Solution Private Limited for the support by providing the BTS data.

REFERENCES

[1]. A.K. Abdelaal, E.F. Mohamed, and A.A ElFergany, Optimal scheduling of hybrid sustainable energy microgrid: a case study for a resort in sokhna, Egypt," *Sustainability,* vol.14, no.12948, 2022

[2]. T.O. Ajewole, O.E. Olabode, K.O. Alawode, and M.O. Lawal, "Small-scale electricity generation through thermal harvesting in rooftop photovoltaic picogrid using passively cooled heat conversion devices," *Environmental Quality Management*, pp.1–8, 2020

[3]. M.Tutak, J. Brodny, and P. Bindzar, "Assessing the level of energy and climate sustainability in the european union countries in the context of the european green deal strategy and agenda 2030," *Energies,* vol.14, pp.1767-1777, 2021

[4]. [4] O.E. Olabode, T.O. Ajewole, I.K. Okakwu, A.S. Alayande, and D.O. Akinyele, "hybrid power systems for off-grid locations: a comprehensive review of design technologies, applications and future trends," *Scientific African*, vol.13, pp. e00884, 2021

[5]. S., Feron, "Sustainability of off-grid photovoltaic systems for rural electrification in developing countries: a review," *Sustainability*, vol.8, no.12, pp.1326, 2016

[6]. F. Martins, P. Moura, and A.T. Almeida, "The role of electrification in the decarbonization of the energy sector in portugal," *Energies,* vol.15, no.5, pp.1759, 2022

[7]. J.O. Aremu, "Epileptic electric power generation and supply in Nigeria: causes, impact and solution," *Journal of Contemporary Research in Social Sciences*, vol.1, pp.73-78, 2019

[8]. The Guardian Newspaper: The growth of smartphone usage in Nigeria. Available at: https://guardian.ng/technology/the-growth-of-smartphone-usage-in-nigeria/ (Accessed on 31st Jan., 2024).

[9]. The state of mobile internet connectivity 2021. Available at: https://www.gsma.com/r/wp-

content/uploads/2021/09/The-State-of-Mobile-Internet-Connectivity-Report-2021.pdf.(Accessed on 31st January, 2024).

[10]. G. Iazeolla, "Power management of base transceiver stations for mobile networks," *Network and Communication Technologies,* vol.1, pp.1-15, 2022.

[11]. G. Piro, M. Miozzo, G. Forte, N. Baldo, L.A. Grieco, G. Boggia and P.H. Dini, "Powered by renewable energy sources: sustainable next-generation cellular networks," *Internet Comput. IEEE*, vol.17, pp. 32–39, 2013

[12]. Nigeria Communications Commission: 3G and 4G Telecoms towers in Nigeria. Available at: https://ncc.gov.ng/media-centre/news-headlines/937-3g-4g-telecom-towers-in-nigeria-now-53-460 danbatta#. (Accessed on 31st January 2024).

[13]. I.K. Okakwu, O.E. Olabode, A.S. Alayande, O.O. Ade-Ikuesan and A.M. Sulaiman, "Comparative analysis of techno-economic viability of hybrid renewable systems as sustainable alternative for energizing selected base transceiver station in Ogun state, Nigeria," *Mindanao Journal of Science and Technology,* vol.18, pp.16-34, 2020.

[14]. [14] I.K. Okakwu, O.E. Olabode, A.S. Alayande, T.E. Somefun and T.O Ajewole, "Techno-economic assessment of wind turbines in Nigeria*" International Journal of Energy Economics and Policy,* vol.11, no.2, pp.240-246,2021.

[15]. J.O. Eko, and M.C. Paul, "Integrated sustainable energy for sub-saharan africa: a case study of maching a Boma in Malawi," *Energies,* vol.14, pp.6330-6347, 2021.

[16]. M.O. Ukoba, O.E. Diemuodeke, M. Alghassab, H.I Njoku, M. Imran, and Z.A Khan, "Composite multi-criteria decision analysis for optimization of hybrid renewable energy systems for geopolitical zones in Nigeria," *Sustainability,* vol.12, pp.5732-5742, 2020.

[17]. K.A. Ali, M.I. Ahmad and Y. Yusup, "Issues, impacts, and mitigations of carbon dioxide emissions in the building sector," *Sustainability,* vol.12, pp.7427-7437, 2020.

[18]. R. Garcia, and F. Freire, "Marginal life-cycle greenhouse gas emissions of electricity generation in Portugal and implications for electric vehicles," *Resources*, vol.*5*, no.4, pp.1-11,2016.

[19]. D. O. Akinyele, R. K. Rayudu and N. K. C. Nair, "Grid-independent renewable energy solutions for residential use: The case of an off-grid house in wellington, New Zealand,"2015 IEEE-PES Asia-Pacific Power and Energy Engineering Conference (APPEEC), pp. 1-5.

[20]. O.E. Olabode, T.O. Ajewole, I.K. Okakwu, and O.O. Ade-Ikuesan "Optimal sitting and sizing of shunt capacitor for real power loss reduction on radial distribution system using firefly algorithm: a case study of Nigerian system," *Energy Sources, Part A: Recovery, Utilization, and Environmental Effects*, pp.1-13, 2019.

[21]. T.O. Ajewole, O.E. Olabode, O.S. Babalola, and M.O. Omoigui, "Use of experimental test systems in the application of electric microgrid technology across the sub-saharan africa: a review," *Scientific Africa,* vol.8, pp. e00435, 2020.

[22]. B.U., Kansara, and B.R. Parekh, "Dispatch, control strategies and emissions for isolated wind-diesel hybrid power system," *International Journal of Innovative Technology and Exploring Engineering,* vol.2, no.6, pp.152-156, 2013.

[23]. O.E. Olabode, I.K. Okakwu, D.O.Akinyele, T.O. Ajewole, S. Oyelami, and O.V.Olisa, "Effect of ambient temperature and solar irradiance on photovoltaic modules' performance," *Iranica Journal of Energy and Environment,* vol.15, no.4, pp.402-420, 2024.

[24]. D. Akinyele, K. Okakwu, E. Olabode, R. Blanchard, T. Ajewole and C., Monyei, "Integrated TEEP approach to microgrid design and planning with small hydro/solar/diesel resources for standalone application," *e-Prime- Advances in Electrical Engineering, Electronics and Energy*, vol.2, pp.100091, 2022.

[25]. L. Uwineza, H. Kim, J. Kleiss, and C. Ki-Kim, "Technical control and optimal dispatch strategy for a hybrid energy system," *Energies,* vol.15, no. 2744, pp.1-19, 2022.

[26]. S.A. Shezan, M.F. Ishraque, S.M. Muyeen, S.M. Arifuzzaman, L.C. Paul, S.K. Das, and S.K. Sarker, "Effective dispatch strategies assortment according to the effect of the operation for an islanded hybrid microgrid," *Energy Conversion and Management,* vol.14, pp.100192, 2022.

[27]. D. Emad, M.A. El-Hameed, and A.A. El-Fergany, "Optimal techno-economic design of hybrid pv/wind system comprising battery energy storage: case study for a remote area," *Energy Conversion Management*, vol.249, pp. 114847, 2021

[28]. M.F. Ishraque, S.A. Shezan, M.M. Rashid, A.B. Bhadra, M.A. Hossain, R.K. Chakrabortty, M.J. Ryan, S.R. Fahim, S.K. Sarker, and S.K. Das "Techno-economic and power system optimization of a renewable rich islanded microgrid considering different dispatch strategies," *IEEE Access*, vol.1, pp.1-17, 2021

[29]. F.H. Jufri, D.R. Aryani, I. Garniwa and B. Sudiarto, "Optimal battery energy storage dispatch strategy for small-scale isolated hybrid renewable energy system with different load profile patterns," *Energies,* vol.14, no.11, pp. 3139, 2021.

[30]. H. Rezk, B. Alamri, M. Aly, A. Fathy, A.G. Olabi, M.A. Abdelkareem and H.A. Ziedan, "multicriteria decision-making to determine the optimal energy management strategy of hybrid pv–diesel battery-based desalination system," *Sustainability*, vol.13, pp.4202, 2021.

[31]. M.F. Ishraque, S.A. Shezan, M.S. Rana, S.M. Muyeen, A. Rahman, L.C. Paul, and M.S. Islam, "Optimal sizing and assessment of a renewable rich standalone hybrid microgrid considering conventional dispatch methodologies," *Sustainability,* vol.13, pp.12734, 2021

[32]. P. Arévalo, D. Benavides, J. Lata-García, and F. Jurado, "Energy control and size optimization of a hybrid system using various storage technologies," *Sustainable Cities Society,* vol.52, pp.101773, 2020

[33]. K. Murugaperumal, S. Srinivasn and S.G.R.K.D. Prasad "Optimum design of hybrid renewable energy system through load forecasting and different operating strategies for rural electrification," *Sustainable Energy Technologies and Assessments,* vol.37, pp.100613, 2020

[34]. M. Ramesh, and R.P. Saini, "Dispatch strategies based performance analysis of a hybrid renewable energy system for a remote rural area in India," *Journal of Cleaner Production,* vol.259, pp.120697, 2020

[35]. A. Micangeli, D. Fioriti, P. Cherubini, and P. Duenas-Martinez, "Optimal design of isolated mini-grids with deterministic methods: matching predictive operating strategies with low computational requirements," *Energies*, vol.13, pp.4214, 2020.

[36]. A. Aziz, M.Tajuddin, M. Adzman, M. Ramli, and S.Mekhilef, "Energy management and optimization of a pv/diesel/battery hybrid energy system using a combined dispatch strategy," *Sustainability,* vol.11, no.3, pp.683, 2019.

[37]. S.A. Shezan, K.N. Hasan, and M. Datta, "Optimal sizing of an islanded hybrid microgrid considering alternative dispatch strategies," *29th Australasian Universities Power Engineering Conference*, pp.1-6, 2019.

[38]. I.K. Okakwu, O.E. Olabode, O.O. Ade-Ikuesan and A.E. Airoboman, "Sizing an off-grid photovoltaic system and economic comparison with petrol generator using life cycle cost (lcc) approach for a typical rural primary

healthcare center in Nigeria" *Journal of Energy and Safety Technology,* vol.2, no.2, pp.41-47, 2019

[39]. G.K. Koufopoulos, and G.A. Vokas, "Improved design of a hybrid energy system for telecommunication applications," *8th Mediterranean Conference on Power Generation, Transmission, Distribution and Energy Conversion*, pp.1-6, 2012.

[40]. Z. Ismaila, O.A. Falode, C.J. Diji, O.M. Ikumapayi, A.A. Awonusi, S.A. Afolalu, and E.T. Akinlabi, "a global overview of renewable energy strategies," *AIMS Energy*, vol.10, no.4, pp.718–775, 2022.

[41]. Solar panel cost in 2024. Available: solar.com/lear/solar-panel-cost/ Accessed: 20/12/2024.

[42]. [42] 1 kVA Honle Inverter. Available: www.honlenewenergy.en.made-in-china.com Accessed: 20/12/2024

[43]. Deep cycle batteries. 12 V 200 Ah Ritar Battery. www.me3energy.ng Accessed: 20/12/2024

[44]. Natural gas generator. Available: electricgeneratorsdirect.com/power/30-kW-natural-gas-generators.html Accessed: 20/12/2024

[45]. D. Akinyele, T. Ajewole, O. Olabode, and I. Okakwu. "Overview and comparative application of on-grid and off-grid renewable energy systems in modern-day electrical power technology. In: Adaptive Power Quality for Power Management Units using Smart Technologies, " CRC Press, pp. 25-65, 2024.

[46]. I. Lamaamar, A. Tilioua and M. A. H. Alaoui, "Thermal performance analysis of poly c-Si PV module under semi-arid conditions," *Materials Science for Energy Technologies,* vol. 5, pp. 243-251, 2022.

[47]. S. Dubey, J. N. Sarvaiya, and B. Seshadri. "Temperature dependent photovoltaic (PV) efficiency and its effect on PV production in the world- A review, " *Energy Procedia,* vol. 33, pp. 311-321, 2013.

[48]. D. Akinyele, J. Belikov and Y. Levron, "Battery storage technologies for electrical applications: Impact in stand-alone photovoltaic systems," *Energiess*, vol. 10, no. 11, pp. 1760, 2017.

[49]. S. Nyamathulla, and C. Dhanamjayulu. "A review of battery energy storage systems and advanced battery management system for different applications: Challenges and recommendations, " *Journal of Energy Storage*, Vol. 86, Part A, pp. 111179, 2024.

[50]. O. E. Olabode, D. O. Akinyele, T. O. Ajewole, S. O. Omogoye, and A. A. Raji. "Impact of integrating type-1 distributed generation on distribution network using modified genetic algorithm and voltage stability index: A technical and cost-benefit analysis approach," Journal of Engineering and Applied Science vol. 71, pp. 222, 2024.

[51]. H. Ajibade, C. O. Ujah, K. C. Nnkwo et al. "Improvement in battery technologies as panacea for renewable energy crisis," Discovery Applied Sciences, vol. 6, pp. 374, 2024.

[52]. T. Ajewole, O. Olabode, F. Ariyo, D. Akinyele, I. Okakwu, and E. B. Omoniyi. "Conceptual perspective of renewable energy resources: A paradigm shift in combating world climate change. In: Adaptive Power Quality for Power Management Units using Smart Technologies, "; CRC Press, pp. 67-103, 2024.